Relativistic Dynamics of Charged Particles

Samuel James Bader
MIT Department of Physics
(Dated: 3 November 2012)

We examine the dynamics of electrons emitted from the decay of ^{90}Sr and confirm that they do indeed follow the predictions of relativity. This paper begins with a brief comparison of the velocity-momentum-energy relations in both non-relativistic and relativistic physics, discusses the experimental measurement of both quantities for charged particles, and analyzes the resulting velocity-momentum and momentum-energy curves. A quantitative evaluation of the fit to the relativistic model is made by employing it to calculate the charge-mass ratio of the electron, and a difference from the accepted value is attributed to systemic error in the magnetic field.

I. KINETIC RELATIONS

Einstein's theory of special relativity makes several counter-classical predictions regarding the most fundamental quantities in physics. One of these basic differences is the non-linear relationship between the velocity of a particle and its momentum, and the non-quadratic relationship between the momentum and the energy. In non-relativistic physics, the momentum is simply the product of mass and velocity, and the energy is always proportional to the square of momentum or velocity. However, relativistic invariance requires that the definitions of momentum and velocity become more complicated:

Classical	Relativistic
$p = mc\beta$	$p = mc\beta/\sqrt{1-\beta^2}$
$KE = \frac{1}{2}mc^2\beta^2$	$KE = mc^2(\sqrt{1+\left(\frac{p}{mc}\right)^2}-1)$

One can easily see that the momentum and energy both approach the non-relativistic expressions when $\beta \ll 1$. However, in the ulta-relativistic limit of $\beta \sim 1$, the energy becomes linear in momentum, and the momentum approaches infinity, because massive particles cannot travel at the speed of light.

Being such a fundamental violation of the physicist's day-to-day intuition for kinetics, we find it vital to probe these relations experimentally.

II. EXPERIMENTAL SETUP FOR MEASURING THE KINETIC RELATIONS

For our purposes, we will use electrons from the radioactive decay of ^{90}Sr/^{90}Y. This source provides a spread of energetic electrons (up to .546MeV from the Strontium, and up to 2.27MeV from the Yttrium, according to [1]). In order to simultaneously determine the various kinetic quantities, we subject the electrons to two sequential regions of electromagnetic field configurations, ending with detection by a PIN diode (see Figure 1). The entire procedure is conducted in a vacuum ($\sim 10^{-4}$ torr) to avoid scattering from air.

The first region is a homogenous magnetic field, which is provided by a spherical current distribution surrounding the electron trajectory in Figure 1. Given a fixed current level, the magnetic field is tested with Hall gaussmeters to be homogenous to within about 1%. Electrons in a magnetic field undergo uniform circular motion with a radius, ρ, dependent on the strength of the magnetic field, B, and the magnitude of their momenta $\vec{p}$, as given in (1).

$$|\vec{p}| = \frac{e\rho B}{c} \tag{1}$$

We fix a magnetic field value. ρ then determined by the momentum. Obstructive baffles, with a narrow slit 90° from the source along the desired ρ-circle, block electrons with trajectories far from the desired radius of curvature, and reduce background counts from electrons bouncing around in the apparatus. A narrow entrance to the next stage of the electron trajectory, which is 180° from the source around the desired ρ-circle, allows the passage of only electrons travelling with a radius of approximately ρ, thus selecting only a tight range of momenta. For this experiment, $\rho = 40.6 \pm .4$cm and the width of the next stage is $.180 \pm .003$cm.

This next stage is two parallel plates ($.180 \pm .003$cm apart, as mentioned) held at a high potential difference (kilovolts). The voltage is set by a high-voltage power source, and monitored throughout the run by a separate multimeter. In order for an electron to pass through undeflected, the electric and magnetic forces upon it must cancel, which selects the velocity as in (2).

$$\beta = \frac{E}{B} \tag{2}$$

where the electric field E is calculated as the voltage applied divided by the plate separation.

So the only electrons passing through to the rear of the plates should be those with momentum $e\rho B/c$ and velocity E/B. Finding the E and B values which allow for the passage of significant counts of electrons thus relates the momenta and velocity. However, we can also measure the energy at this point by placing a PIN diode at the

rear of the plates. When an electron strikes the diode, it will emit a charge pulse proportional to the energy which the electron deposits. This is amplified as a voltage signal and sent to a multi-channel analyzer (MCA), which counts the pulses it receives, binned by the voltage. Thus the data read out from the MCA is effectively a histogram over energies of the incoming electrons.

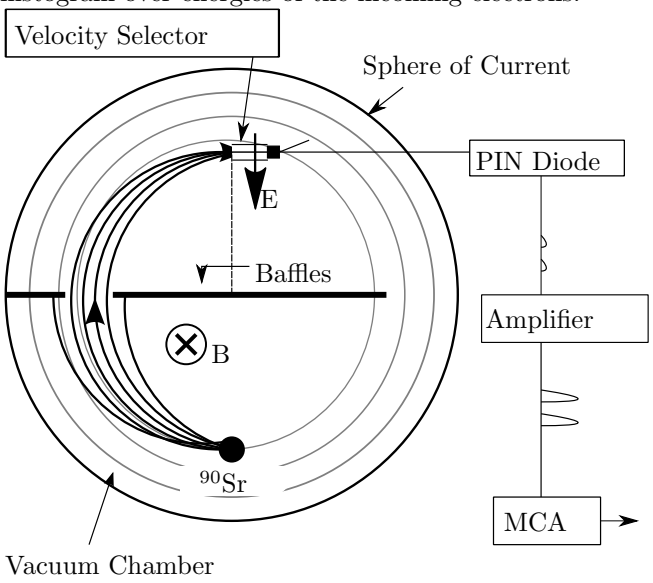

FIG. 1: Radiated electron pass through a magnetic field (momentum selector) and a velocity selector, before striking the PIN diode. The MCA records electron hits.

III. CALIBRATIONS

In order to determine the energies of the electron beams from an MCA readout, the energies of the MCA bins must be determined by calibration with beams of known energy. For that, we place a ^{133}Ba/^{133}Cs source, whose spectrum contains several well-known lines, in the apparatus and recorded the spectrum over several days ($\sim$ 135 hours). We matched seven of the most well-defined peaks on the MCA readout to seven lines in the ^{133}Ba/^{133}Cs decay spectrum, as depicted in Figure 2.

Each day of the experiment, we took a shorter calibration curve to ensure that the bin-energy relation did not change by a significant amount.

IV. PROCEDURE

We chose several values of magnetic field at which to measure (60G, 70G, 80G, 85G, 95G, 100G, 105G), limited by increasing noise at lower magnetic fields and difficulty sustaining higher magnetic fields due to ohmic heating in the apparatus. At each magnetic field, we tested several values of the voltage across the plates, recording the MCA readout for each (over a 100s interval). For each voltage, we sum the counts per second, thus obtaining a voltage vs total counts curve, such as that in Figure 3.

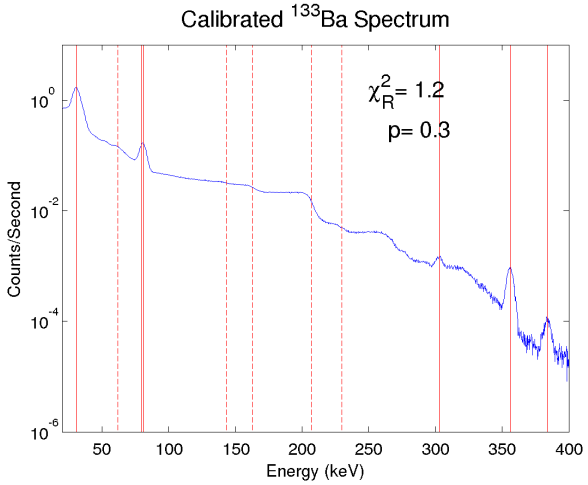

FIG. 2: The blue curve is the spectrum read from the MCA (error bars would be too small to appear on the plot). The energies on the horizontal axis are linearly fitted so that peaks in the MCA spectrum match ^{133}Ba/^{133}Cs transitions. The solid red lines are the locations of the seven transition energies used in the fit. Notice that the low χ^2 supports our linear calibration. Additionally, the dashed lines are Compton edges predicted from other transitions (see [2]).

Ideally, with the magnetic field selecting some specific momentum, there should be some voltage which selects for the corresponding velocity, and that voltage should give the greatest count rate on the MCA. All of the curves looked roughly symmetric to the resolution of our data, so, to determine the "best" voltage, we fit Gaussians to each and extracted the fitted center, as depicted in Figure 3. Dividing the "best" voltage by the distance between the plates gives the electric field experienced by the electrons.

For each magnetic field, at the determined voltage, we take a longer run (300s) in order to get a clear energy peak on the MCA (example shown in Figure 4). These peaks have no well-defined shape, so we take centroids to determine the central energy of the electron beam.

At the end of this procedure we have, for each value of the magnetic field (from which we can determine momentum), a corresponding electric field (which enables us to then determine velocity), and a peak on the MCA (from which we can determine energy).

V. DATA AND ANALYSIS

From the magnetic field, electric field, and energies measured, we can determine, for each run, the velocity, momentum, and energy of the electrons (using the formulae from the introduction). Here we examine those

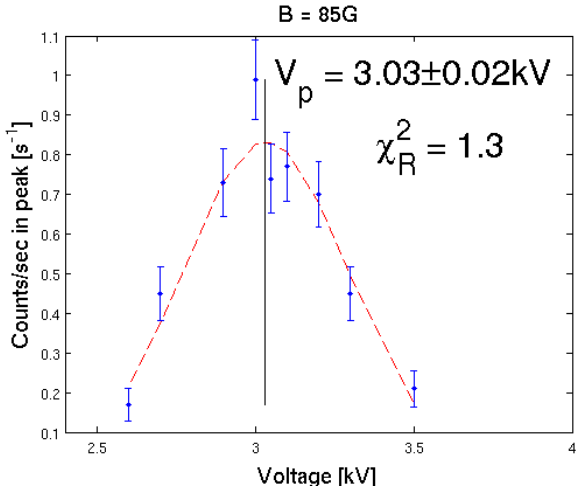

FIG. 3: This Gaussian fit demonstrates how the "best" voltage was determined for the 85G run.

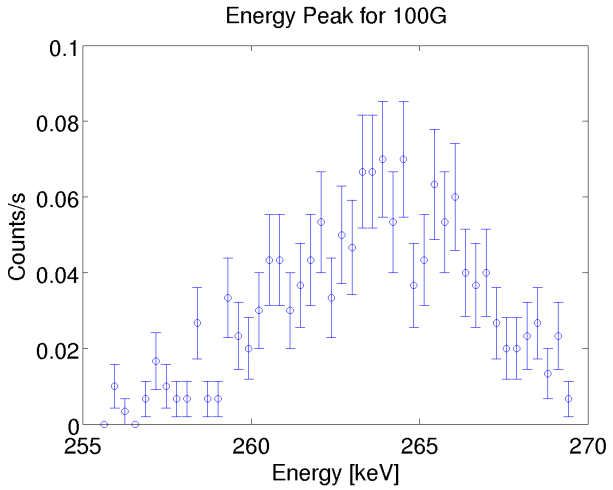

FIG. 4: The energy peak recorded by the MCA for a 300 second run at 100G

curves.

For visual demonstration, the experimental relationship between energies and momenta is given in Figure 5 and between momenta and velocities in Figure 6. We see immediately that our data lie significantly closer to the relativistic curves, and are certainly not described by the non-relativistic line. It is also clear that the data are systematically shifted slightly from the relativistic curves, which we will discuss in our errors.

Testing our results numerically, we will calculate the charge-mass ratio of the electron. From the momentum velocity relations and the relations with the electromagnetic fields, one can derive the following two determinations of e/m.

Classical	Relativistic
$\frac{e}{m} = \frac{\beta}{B\rho/c^2}$	$\frac{e}{m} = \frac{\beta/\sqrt{1-\beta^2}}{B\rho/c^2}$

By evaluating those expressions at each data point and averaging the results (weighting by uncertainties), one finds the following values of the charge-mass ratio

Classical	Relativistic
$\frac{e}{m} = (3.48 \pm .03_{\text{stat}})$	$\frac{e}{m} = (4.76 \pm .06_{\text{stat}})$
$\times 10^{17}$esu/g	$\times 10^{17}$esu/g

In Figures 7 and 8, we plot the numerators and denominators of those ratios. We see that the non-relativistic prediction is a terrible fit ($\chi^2_R = 18.16$) and the relativistic prediction is a solid fit ($\chi^2_R = 1.02$). However, the known value of e/m is actually 5.27×10^{17}esu/g. The relativistic calculation is much closer; but both values are many (statistical) standard deviations away. This appears to be due to the same systematic error which causes the shifts in Figures 5 and 6 and will be accounted for in our sources of error.

VI. ERROR

The errors in the electric field determinations are given by the parameter uncertainties in the voltage fits (discussed in the procedure), with an additional error from the uncertain plate distance. Together, the electric field error amounts to about 2% for each data point. The statistical uncertainty in the magnetic field (from measurement errors) was taken to be 1%.

However, the systemic uncertainties, specifically in the magnetic field, are more worrisome. They are not large comparatively, but because systematic uncertainties do not reduce with averaging, they seem to have shifted our answers significantly. First of all, the ∼1% inhomogeneity in the magnetic field means that the magnetic field we measure from the center of the sphere may not be that experienced by the electrons. Additionally, we could only calibrate the Hall gaussmeters to within 2%, and, on the fourth day of the the experiment (Oct 18), we switched gaussmeters, which changes the systemic effects for certain data points. The switching of magnetometers actually allows us to observe easily what effect this could have had. Reexamining the data in Figure 6, but paying attention to the date on which each data point was collected, we see that the data from the 18$^{\text{th}}$ is noticeably further from the prediction than data on the 10$^{\text{th}}$ or 16$^{\text{th}}$.

In fact, in order to get a crude estimate of how this systematic uncertainty could have affected the experiment, we can adjust our magnetic field values by a worst-case plausible error. That is, we assume our magnetic field

measurements overstated B by 2G. If we simply repeat the above analysis, we find a new value of e/m for the relativistic case.

$$\frac{e}{m} = (5.20 \pm .07_{\text{stat}}) \times 10^{17}\text{esu/g}$$

This value is now within one standard deviation of the accepted value (and the non-relativistic value remains tens of standard deviations away). The $\chi^2_R = 1.22$ of the new fit is not significantly different, so we are comfortable that our conclusions, if not the specific value of e/m, are robust against this error. Assuming the correctness of the model, this would indicate that our field measurement was most likely off by an order of 2G.

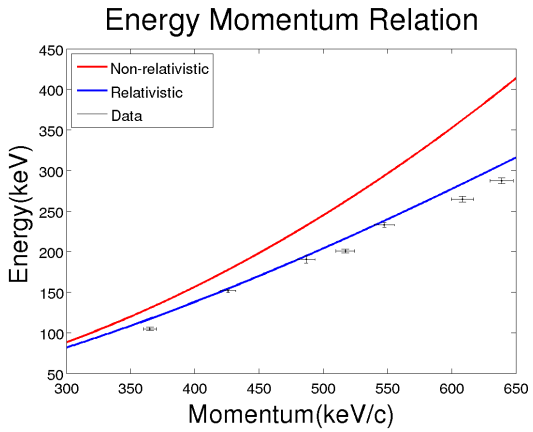

FIG. 5: The energy-momentum curve is clearly non-classical.

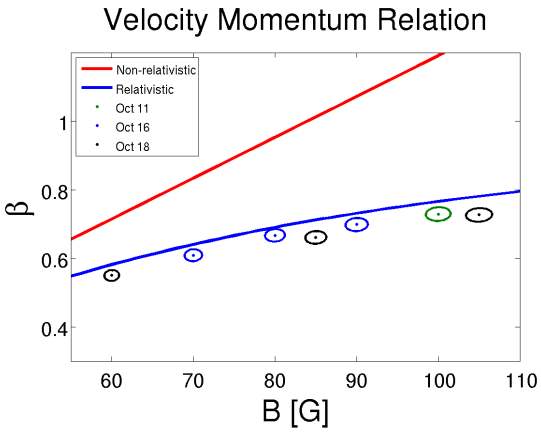

FIG. 6: The velocity-momentum curve is also clearly non-classical.

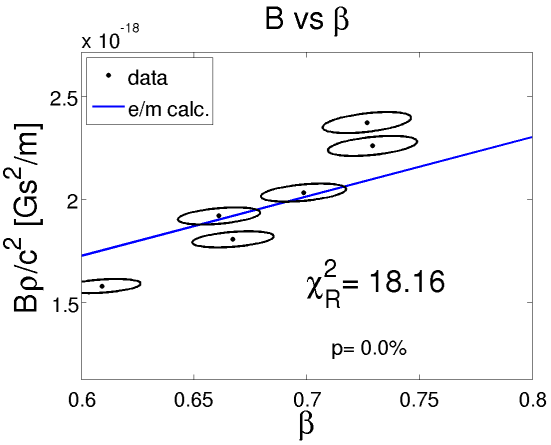

FIG. 7: The non-relativistic momentum-velocity relation is a terrible fit.

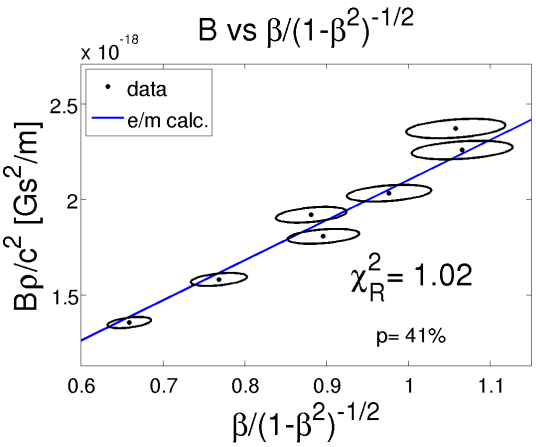

FIG. 8: The relativistic relation fits the data very well.

VII. CONCLUSION

This experiment provided a testbed for probing the relativistic dynamics of electrons. By analyzing the relations of the various kinetic variables, we found two results. First, we found a determination of the electron charge-mass ratio. Our intial value was statistically not in agreement with the known value; however, if the systematic uncertainty in the magnetic field could be eliminated, then, we expect, based on the above error analysis, that our value would be acceptable. More broadly, we found that, entirely regardless of the magnetic field uncertainty, the kinetics of electrons from radioactive decay are not appropriately described by non-relativistic dynamics, and do indeed require relativistic treatment.

[1] "Relativistic Dynamics" Lab Guide. MIT Department of Physics. http://web.mit.edu/8.13/www/09.shtml

[2] Melissinos, Adrian. *Experiments in Modern Physics*. Academic Press, 1966.